

Climate-driven processes of hillslope weathering

Jean L. Dixon^{1*}, Arjun M. Heimsath^{1*}, James Kaste^{2*}, and Ronald Amundson^{3*}

¹School of Earth and Space Exploration, Arizona State University, 548 Physical Sciences F-wing, Tempe, Arizona 85287, USA

²Department of Geology, College of William and Mary, 217 McGlothlin-Street Hall, Williamsburg, Virginia 23187, USA

³Department of Environmental Science, Policy and Management, University of California–Berkeley, 137 Mulford Hall, Berkeley, California 94720, USA

ABSTRACT

Climate controls erosion and weathering on soil-mantled landscapes through diverse processes that have remained difficult to disentangle due to their complex interactions. We quantify denudation, soil and saprolite weathering, and soil transport near the base and crest of the western slope of the Sierra Nevada to examine how large differences in climate affect these processes. Depth profiles of fallout radionuclides and field observations show relative differences in erosion and weathering processes at these two climatically diverse sites, and our data suggest fundamentally different patterns of soil production and transport mechanisms: biotically driven soil transport at low elevation, and surface erosion driven by overland flow at high elevation. Soil production rates from cosmogenic ¹⁰Be decrease from 31.3 to 13.6 m/Ma with increasing soil depth at low elevation, but show uncertain depth dependence at the high elevation site. Our data also show a positive correlation between physical erosion and saprolite weathering at both sites. Highly weathered saprolites are overlain by weakly weathered and rapidly eroding soils, while chemically less depleted saprolites are overlain by slowly eroding, more weathered soils. Our data are among the first to quantify the critical role of saprolite weathering in the evolution of actively eroding upland landscapes, and our results provide quantitative constraints on how different climates can shape hillslopes by driving processes of erosion and weathering.

INTRODUCTION

Soils are a dynamic interface between the atmosphere, biosphere, and Earth's surface; chemical and physical processes within soils should therefore express the influence of climate on landscape evolution. Climate directly influences the processes affecting hillslope soils by (1) controlling vegetation and fauna, which physically move and mix soil and influence acidity, and (2) affecting chemical weathering by driving soil temperature and water through-flow rates. The effects of temperature and precipitation on chemical weathering are studied through modeling (e.g., Casey and Sposito, 1992), laboratory experiments (e.g., White and Brantley, 2003), examination of soil and stream solutes (e.g., White and Blum, 1995), and the measurement of immobile elements in soil (e.g., Riebe et al., 2004). Soil transport mechanisms also respond to climate and control rates of erosion and chemical weathering, yet an explicit consideration of the role of individual transport processes has not been widely integrated into denudation and/or weathering analyses of soil-mantled terrain.

Potential links between climate and long-term erosion on nonglaciated landscapes are increasingly being examined (e.g., Riebe et al., 2004), but the relationships remain elusive due to limited field data. Attempts to correlate hillslope response to climate have focused primarily on rates of landscape change, and few have quantified the mechanisms by which climate influences erosion and weathering processes (e.g., von Blanckenburg, 2006). Furthermore, we are aware of no studies that have specifically examined links between climate, saprolite weathering, and erosion. Here we employ a novel combination of established methods to quantify

chemical weathering in both the soil and saprolite, and link weathering to rates and processes of downslope soil transport. We quantify soil production rates using the in situ-produced cosmogenic radionuclide (CRN) ¹⁰Be, and chemical weathering using bulk chemical analyses of soil, saprolite, and bedrock. In addition, we use field metrics and fallout-derived ²¹⁰Pb and ¹³⁷Cs in soil profiles to identify transport processes. These combined methods help reveal the underlying differences in weathering and erosion for two landscapes at the ends of a large climate gradient.

STUDY SITES AND APPROACH

The study sites are the end members of a well-studied climosequence along the western slope of the Sierra Nevada range in California (United States). Previous work focused on general trends in soil formation and rates of carbon cycling along the climate gradient (Dahlgren et al., 1997; Trumbore et al., 1996). In this study, a low-elevation grassland site (Blasingame, BG; ~220 m) and a sparsely vegetated, high-elevation subalpine site near the Sierran crest (Whitebark, WB; ~2990 m) are separated by ~2900 m in elevation and 64 km (Fig. 1). Both sites are underlain by unglaciated granodiorite of similar composition (Bateman and Lockwood, 1970, 1976). Annual precipitation increases from 37 to 106 cm and average temperature decreases from 16.6 to 3.9 °C with elevation (Prism database; PRISM Climate Group, 2008). Helium thermochronometry (e.g., Clark et al., 2005) and CRN-dated cave sediments (Stock et al., 2005) suggest that rapid river incision in the Sierra Nevada is likely associated with Cenozoic uplift; however, much of the upland soil mantled-landscape has not responded to this forcing (e.g., Clark et al., 2005). We chose sites with minimal differences in lithology, tectonics, and recent glaciation to isolate the role of climate on erosion and weathering processes in the region, and use the end members along the transect to take advantage of the maximum available climate signal.

We sampled saprolite beneath soil at selected hillslopes, along downslope transects from crest to swale, and measured ¹⁰Be in saprolite to determine soil production rates (P_{soil}) (e.g., Heimsath et al., 2005). We measured zirconium concentrations in soil, saprolite, and rock using pressed pellet X-ray fluorescence, and calculated fractional chemical losses in soil and saprolite using the chemical depletion fraction (CDF) (Riebe et al., 2004). We calculated the CDF_{total} (relative dissolved mass loss of soil relative to bedrock), $CDF_{saprolite}$ (from [Zr] in saprolite relative to rock) and CDF_{soil} (from [Zr] in soil relative to saprolite). The sites examined have divergent planform topography, which lacks the complication of an upslope contribution of previously weathered material (Yoo et al., 2007). Thus, in these settings, the CDF largely reflects chemical weathering during soil production. Chemical weathering rates of soils (W_{soil}) and saprolites ($W_{saprolite}$), and physical erosion rates were determined by coupling the CDF with CRN-derived denudation rates (e.g., Riebe et al., 2004) (see GSA Data Repository¹ for equations and derivations).

We examined soil mixing and transport processes using fallout radionuclides and by observations of biological activity in the field. We mea-

*E-mails: jean.dixon@asu.edu; arjun.heimsath@asu.edu; jmkaste@wm.edu; earthy@nature.berkeley.edu (Amundson).

¹GSA Data Repository item 2009248, nuclide activity data and modeled diffusion coefficients, is available online at www.geosociety.org/pubs/ft2009.htm, or on request from editing@geosociety.org or Documents Secretary, GSA, P.O. Box 9140, Boulder, CO 80301, USA.

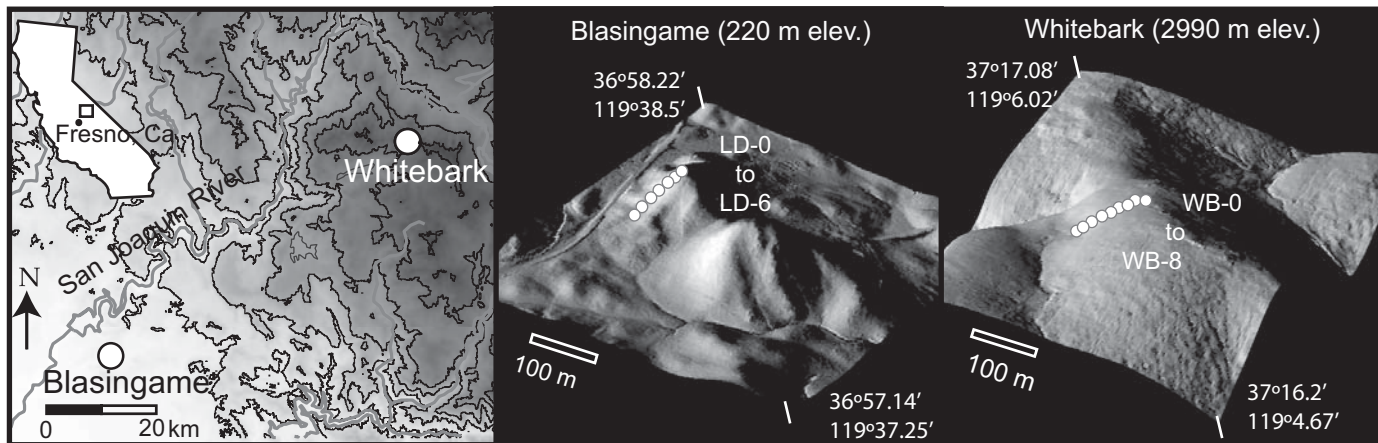


Figure 1. Location of field area showing low-elevation grassland site, Blasingame, and high-elevation subalpine site, Whitebark. Light ranging and detection data (provided by National Center for Airborne Laser Mapping) were used to derive slope and curvature and produce shaded relief images.

sured $^{210}\text{Pb}_{\text{excess}}$ (shortened here to ^{210}Pb) and ^{137}Cs nuclide activities with depth and calculated total inventories to gain insight into mixing (e.g., Kaste et al., 2007) and soil erosion mechanisms (e.g., Wallbrink and Murray, 1993; Kaste et al., 2006). The nuclide profile depth was defined as the soil depth at which >95% of the cumulative nuclide activity, or inventory, was obtained. We used nuclide profiles to determine the degree of physical mixing, and calculated a diffusion coefficient by the best-fit exponential curve to an advection-diffusion equation (Kaste et al. 2007) (see the Data Repository and Fig. 2 for equations).

We determined the average fractional vegetative cover from photos to estimate soil exposure to raindrop splash and resistance to overland flow. Gopher and ground squirrel burrowing activity at each site was measured by recording burrow number and size at the ground surface within a 2 m swath extending 54–114 m along three contour parallel transects and one profile transect. We calculated a surface area expression of burrowing activity per hillslope area by multiplying burrow density by burrow diameter (see the Data Repository).

PATTERNS OF EROSION AND CHEMICAL WEATHERING

Hillslope soil production rates average $82 \pm 10 \text{ t/km}^2/\text{a}$ ($37 \pm 4 \text{ m/Ma}$; mean \pm standard error) at the low-elevation BG site and $52 \pm 5 \text{ t/km}^2/\text{a}$ ($24 \pm 2 \text{ m/Ma}$) at the high-elevation WB site. At BG, soil production rates decrease with increasing soil thickness (Fig. 2A) and distance from the slope crest (Fig. 2B), as observed in other temperate landscapes (e.g., Heimsath et al., 2005). This relationship is not shown at WB.

Chemical weathering results in an average net loss of $24\% \pm 4\%$ of the soil mass at both sites, calculated as the average CDF_{soil} , and CDF values are not significantly different at the two sites. Dahlgren et al. (1997) observed that the clay content of the low-elevation soils exceeds that of WB soils by a factor of two. This suggests a discrepancy in how soil weathering intensity is recorded by CDF and clay abundance. The CDF quantifies net elemental losses; however, secondary mineral formation is the balance between chemical dissolution of primary minerals and the leaching of weathering products. Potential mass loss may exceed net mass loss at low elevation, due to secondary mineral development and retention, in agreement with previous observations of the low leaching potential of clay minerals in these soils compared to high-elevation soils (Dahlgren et al., 1997). Thus, the total chemical alteration at the BG site is greater despite similar net losses to the WB site.

At both sites, CDF_{sap} data indicate that saprolite weathering is a large portion of the total weathering losses, averaging $31\% \pm 4\%$ and reaching

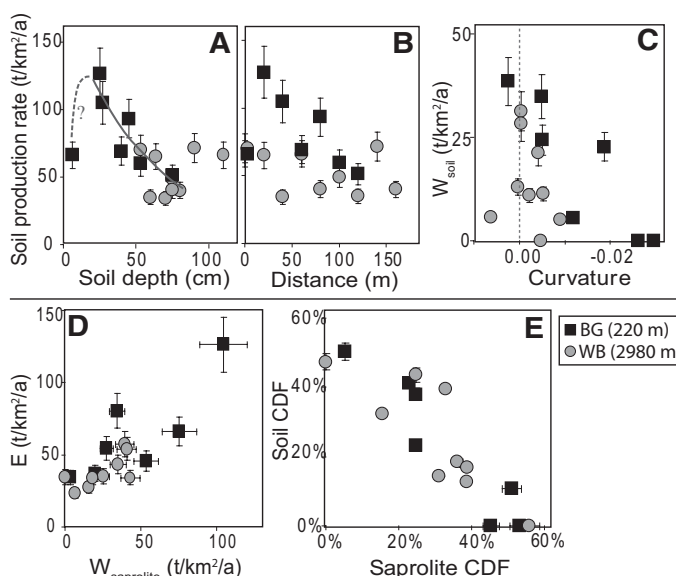


Figure 2. Average ^{10}Be -derived soil production rates (P_{soil}) are higher at Blasingame (BG) than Whitebark (WB) (one-tailed t -test, $t = 7.28$, $p = 0.02$). **A:** At BG, these rates decrease with soil thickness ($P_{\text{soil}} = 77e^{-0.017h}$, $r^2 = 0.81$). **B:** At BG, these rates decrease with distance from crest ($r^2 = 0.81$, $p < 0.01$). Hill crest alone deviates from these trends, suggesting either exponential soil production function with hill crest held up by slower eroding feature such as emergent tor, or humped production function, whereby production rates peak at some finite soil thickness. **C:** Soil chemical weathering rates (W_{soil}) decrease with increasing convexity (negative curvature) at BG ($r^2 = 0.75$, $p = 0.05$), and insignificantly at WB ($r^2 = 0.31$, $p = 0.19$). **D:** Physical erosion rates increase with chemical weathering rate of saprolite ($W_{\text{saprolite}}$) at both sites (all data: $r^2 = 0.68$, $p = 0.02$; BG: $r^2 = 0.48$, $p = 0.04$; WB: $r^2 = 0.69$, $p < 0.01$). Average rates of erosion are faster at warmer and drier BG (one-tailed t -test, $p = 0.04$), compared to colder and wetter WB, although saprolite weathering rates are not significantly different ($p = 0.13$). **E:** Soil and saprolite weathering extents, shown by chemical depletion fractions (CDF), are negatively correlated (all data: $r^2 = 0.78$, $p < 0.01$; BG: $r^2 = 0.87$, $p < 0.01$; WB: $r^2 = 0.69$, $p < 0.01$).

values as high as 56% of the original rock mass. Saprolite weathering rates average $46 \pm 13 \text{ t/km}^2/\text{a}$ at BG and $25 \pm 5 \text{ t/km}^2/\text{a}$ at WB. Physical erosion rates at low and high elevations average $64 \pm 12 \text{ t/km}^2/\text{a}$ and $38 \pm 4 \text{ t/km}^2/\text{a}$, respectively. At BG, soil chemical weathering rates decline

with increasing convexity (Fig. 2C). Furthermore, physical erosion and saprolite weathering rates at both sites are positively correlated (Fig. 2D), and a strong negative relationship exists between the chemical weathering extents of soils and saprolites (Fig. 2E). We explore implications of these data following the quantification of transport processes.

SEDIMENT TRANSPORT PROCESSES

Fallout radionuclide activity-depth profiles and field observations reveal distinct differences in sediment transport processes at the climate end members. Vegetative density is lowest at the high-elevation WB site, with an average of 83% bare soil versus 4% at the BG site. Low vegetative cover and high precipitation at WB result in low soil resistance to surface water flow and raindrop splash (e.g., Prosser and Dietrich, 1995). Rills began ~40 m downslope from the crest at WB. These have an upslope spacing of 23 m decreasing to an average spacing of 9 m at ~60 m from the slope crest. No rilling was evident at BG. At both sites, bioturbation is evident in soils, and gopher burrows were observed parallel to the ground surface and as deep as the soil-saprolite interface. Mapping gopher burrow density indicates that the burrowing activity at WB is 53% that of BG (Table DR6 in the Data Repository).

Penetration depths of ^{210}Pb and ^{137}Cs increase linearly with burrowing activity at both sites (Fig. 3A), suggesting that bioturbation (through physical transport and altered hydrology) redistributes nuclides to depth in the soil. Assuming that nuclide profiles form primarily by diffusion-like processes, the average diffusive mixing coefficient of soils is $0.28 \pm 0.05 \text{ cm}^2/\text{a}$ at BG, greater than the average $0.15 \pm 0.02 \text{ cm}^2/\text{a}$ at WB (Fig. 2B). The ^{210}Pb inventories do not vary consistently with topography at BG; however, at WB, inventories are lowest where slopes are steepest and have the greatest upslope contributing area (Figs. 3C and 3D). Upslope contributing area has the strongest negative correlation with nuclide inventory at WB, suggesting that soil loss scales with discharge (e.g., Kaste et al., 2006). This correlation, in agreement with the observation of rills, shows that overland flow plays an important role in soil transport at WB.

While overland flow may play a dominant role in sediment transport at WB, it likely has little impact on soil production. Spatial patterns of soil production are distinctly different at these sites (Figs. 2A and 2B), and an apparent soil production function at low elevation is consistent with production mechanisms such as rooting and bioturbation, which are expected to be depth dependent (e.g., Gabet et al., 2003). It is possible that the absence of a trend between P_{soil} and depth at WB (Fig. 2A) is due to soil depths temporarily out of local steady state, and the two deepest samples are anomalies in the sampled transect (see the Data Repository and Fig. DR2). More likely, the absence of depth-dependent soil production at WB (Fig. 2A) and the differences in hillslope patterns of erosion and weathering (Figs. 2B and 2C) suggest that a different mechanism is dominant at the high-elevation site. With average annual temperatures of 3.9°C , freeze-thaw may occur at WB; however, this process is also likely depth dependent (e.g., Anderson, 2002). Furthermore, freeze-thaw are likely not dominant soil production or transport processes, given that rills are prominent on the land surface and that soil thicknesses are typically $>1 \text{ m}$. Biotite hydration and oxidation may occur at depth in saturated soils during spring snowmelt; however, our data do not speak directly to this mechanism and further research is needed to explain what processes ultimately create these thick high-elevation soils.

MECHANISTIC CONTROLS ON WEATHERING AND EROSION

Chemical weathering facilitates physical erosion by the dissolution of primary minerals, reducing the competence of rock and increasing erodability. Our data are among the first to quantify links between saprolite weathering and physical erosion. Physical erosion rates increase with

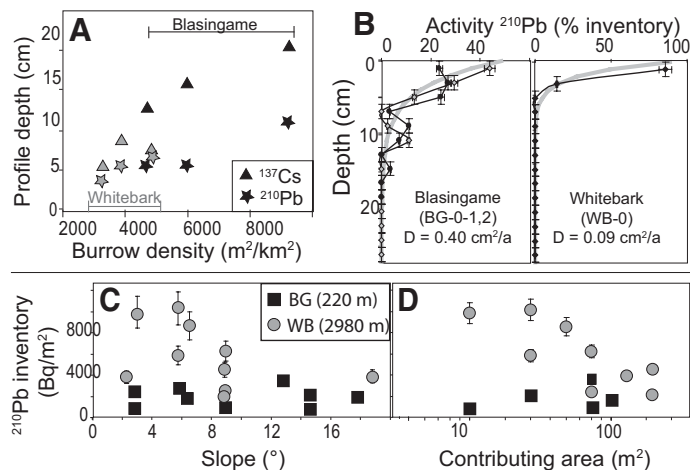


Figure 3. A: Surface burrowing activities from three transects at Blasingame (BG) and Whitebark (WB) increase with associated profile depths for fallout nuclide ^{210}Pb ($r^2 = 0.95$, $p < 0.01$) and ^{137}Cs ($r^2 = 0.85$, $p < 0.01$). Profile depth is defined as soil depth at 95% cumulative nuclide inventory. **B:** Fallout profiles show nuclide activity versus depth for hill crests at BG (two profiles shown are 2 m apart) and WB (one profile) and are deeper at BG. We calculated diffusion-like mixing coefficients (D) for each profile (shown by broad gray line) by

best fit to the diffusion equation: $a(z) = a_0 \cdot \exp\left[\frac{V - \sqrt{V^2 + 4\lambda D}}{2D}(z)\right]$,

where $a(z)$ and a_0 are nuclide activity at depth (z) and surface, respectively, and λ is nuclide decay. Here, we assume that advection velocity (V) is zero. Diffusive mixing coefficients of hill crests are shown, and average hillslope values at each site are $0.28 \pm 0.05 \text{ cm}^2/\text{a}$ at BG and $0.15 \pm 0.02 \text{ cm}^2/\text{a}$ at WB. Also shown are inventories of $^{210}\text{Pb}_{\text{excess}}$ and ^{137}Cs for downslope soils at low-elevation BG site (gray squares) and high-elevation WB site (black circles). Inventory data points reflect those calculated from individual soil profiles, and activities of additional bulk soil samples gathered downslope. **C:** Nuclide inventories at high elevation are lower at high slopes; however, no statistically significant correlation exists. **D:** At BG, inventories do not change markedly, while at WB, nuclide inventories decrease with distances downslope and increasing contributing area ($r^2 = 0.63$, $p = 0.01$). Symbols contain error if not otherwise labeled. Nuclide activities were measured using gamma-ray spectrometry on a broad energy germanium detector at Dartmouth College (Hanover, New Hampshire). Downslope profiles of $^{210}\text{Pb}_{\text{excess}}$ for each pit, including modeled mixing coefficients, are provided in Data Repository (see footnote 1).

saprolite weathering rates (Fig. 2D). These data suggest that physical erosion is dependent on the chemical weathering extent and rate of bedrock, because weathered saprolite is more easily detachable and mobilized into the overlying soil column. Furthermore, soil chemical weathering rates at low elevation decline with increasing convexity (Fig. 2C), and the intensities of chemical weathering in soils and saprolites are inversely related (Fig. 2E). Soil weathering may be low where saprolite weathering is high due to faster erosion that reduces soil residence times (e.g., Anderson et al., 2002). As water and sediment are shed off divergent areas of the landscape, decreased water-soil interaction could further result in decreased chemical weathering of soils. Conversely, similar $\text{CDF}_{\text{total}}$ across the Sierras may support the idea that weathering of parent bedrock is limited by the supply of fresh minerals, rather than reaction rates (e.g., Riebe et al., 2001; West et al., 2005). Saprolite weathering in the Sierras, indicated by saprolite CDFs and rates, is controlled by processes not clearly identified from our study, but is possibly linked to climate, moisture availability, and hillslope morphology. Our data suggest that soil weathering is limited by the availability of fresh minerals, and is therefore low when saprolite has previously depleted this supply.

CONCLUSION

We explored the expression of climate on two diverse landscapes by explicitly quantifying the processes and rates of hillslope erosion and weathering. Two principal findings emerge from our data. First, we quantified different rates and processes of soil transport and production at the two sites considered to be end members of a well-studied climosequence. Rates of soil production, erosion, and chemical weathering in saprolite are nearly two times higher at the low-elevation site than at the cooler subalpine site. Measurements of diffusive soil mixing suggest that bioturbation may be twice as important at BG than WB, in agreement with gopher burrow densities. Soil production rates decrease with soil thickness in this vegetated low-elevation site (Fig. 2A), as observed at similar bioturbated grassland landscapes (e.g., Heimsath et al., 2005). At WB, exposed soil, sparse vegetative cover, the presence of rills, and nuclide inventories that increase with contributing area (Fig. 3C) indicate the importance of advective soil transport processes such as overland flow. These results quantify how different climates shape landscapes by influencing the rates and patterns of chemical weathering and soil transport processes.

Second, and perhaps most important, our data show strong feedbacks between physical erosion and chemical weathering at both study sites, despite broad differences between the climates and the soil production and transport mechanisms. Others have reported positive correlations between soil chemical weathering and erosion and have suggested that physical erosion sets the pace of chemical weathering (e.g., Riebe et al., 2004) in soil-mantled terrain. Our data indicate that saprolite weathering and erosion are positively linked (Fig. 2D), and soil weathering is reduced where both saprolite weathering (Fig. 2E) and landscape convexity (Fig. 2C) are high. In summary, our data suggest that saprolite weathering controls erosion and weathering of the overlying soil by depleting primary minerals, decreasing rock competence, and increasing the mobility of weathered material. Because chemical weathering of the saprolite accounts for such significant mass loss from these landscapes, we suggest that not accounting for it leads to missing a critical aspect of erosion-weathering feedbacks.

ACKNOWLEDGMENTS

This work was funded by a National Science Foundation EAR CAREER grant (Heimsath), Sigma Xi Grants in Aid of Research, and the Dartmouth College Department of Earth Sciences. Light ranging and detection data were provided by the National Center for Airborne Laser Mapping. B. Burke, A. Bowling, and L. Hester provided assistance in the field and laboratory. Tim Allen at Keene State University helped with X-ray fluorescence analyses. We thank M. Blasingame and K. Lowe for field support and access to their property. This manuscript benefited greatly from helpful and insightful comments by D.R. Montgomery, R.S. Anderson, G.E. Hilley, and an anonymous reviewer.

REFERENCES CITED

- Anderson, R.S., 2002, Modeling the tor-dotted crests, bedrock edges, and parabolic profiles of high alpine surfaces of the Wind River Range, Wyoming: *Geomorphology*, v. 46, p. 35–58, doi: 10.1016/S0169-555X(02)00053-3.
- Anderson, S., Dietrich, W., and Brimhall, G., Jr., 2002, Weathering profiles, mass balance analysis, and rates of solute loss: Linkages between weathering and erosion in a small, steep catchment: *Geological Society of America Bulletin*, v. 114, p. 1143–1158, doi: 10.1130/0016-7606(2002)114<1143:WPMBAA>2.0.CO;2.
- Bateman, P.C., and Lockwood, J.P., 1970, Kaiser Peak Quadrangle, central Sierra Nevada, California—Analytic data: U.S. Geological Survey Professional Paper 644-C, 15 p.
- Bateman, P.C., and Lockwood, J.P., 1976, Shaver Lake quadrangle, west-central Sierra Nevada, California—Analytic data: U.S. Geological Survey Professional Paper 774-D, 20 p.
- Casey, W.H., and Sposito, G., 1992, On the temperature-dependence of mineral dissolution rates: *Geochimica et Cosmochimica Acta*, v. 56, p. 3825–3830, doi: 10.1016/0016-7037(92)90173-G.
- Clark, M.K., Maheo, G., Saleeby, J., and Farley, K.A., 2005, The non-equilibrium landscape of the southern Sierra Nevada, California: *GSA Today*, v. 15, p. 4–10, doi: 10.1130/1052-5173(2005)015[4:TNLOTS]2.0.CO;2.
- Dahlgren, R.A., Boettinger, J.L., Huntington, G.L., and Amundson, R.G., 1997, Soil development along an elevational transect in the western Sierra Nevada, California: *Geoderma*, v. 78, p. 207–236, doi: 10.1016/S0016-7061(97)00034-7.
- Gabet, E.J., Reichman, O.J., and Seabloom, E.W., 2003, The effects of bioturbation on soil processes and sediment transport: *Annual Review of Earth and Planetary Sciences*, v. 31, p. 249–273, doi: 10.1146/annurev.earth.31.100901.141314.
- Heimsath, A.M., Furbish, D.J., and Dietrich, W.E., 2005, The illusion of diffusion: Field evidence for depth-dependent sediment transport: *Geology*, v. 33, p. 949–952, doi: 10.1130/G21868.1.
- Kaste, J.M., Heimsath, A.M., and Hohmann, M., 2006, Quantifying sediment transport across an undisturbed prairie landscape using cesium-137 and high resolution topography: *Geomorphology*, v. 76, p. 430–440, doi: 10.1016/j.geomorph.2005.12.007.
- Kaste, J.M., Heimsath, A.M., and Bostick, B.C., 2007, Short-term soil mixing quantified with fallout radionuclides: *Geology*, v. 35, p. 243–246, doi: 10.1130/G23355A.1.
- PRISM Climate Group, 2008, Prism database: PRISM Climate Group, Oregon State University, created 5 March 2008, <http://prism.oregonstate.edu>.
- Prosser, I.P., and Dietrich, W.E., 1995, Field experiments on erosion by overland-flow and their implication for a digital terrain model of channel initiation: *Water Resources Research*, v. 31, p. 2867–2876, doi: 10.1029/95WR02218.
- Riebe, C.S., Kirchner, J.W., Granger, D.E., and Finkel, R.C., 2001, Strong tectonic and weak climate control of long-term chemical weathering rates: *Geology*, v. 29, p. 511–514, doi: 10.1130/0091-7613(2001)029<0511:STAWCC>2.0.CO;2.
- Riebe, C.S., Kirchner, J.W., and Finkel, R.C., 2004, Erosional and climatic effects on long-term chemical weathering rates in granitic landscapes spanning diverse climate regimes: *Earth and Planetary Science Letters*, v. 224, p. 547–562, doi: 10.1016/j.epsl.2004.05.019.
- Stock, G.M., Anderson, R.S., and Finkel, R.C., 2005, Rates of erosion and topographic evolution of the Sierra Nevada, California, inferred from cosmogenic ²⁶Al and ¹⁰Be concentrations: *Earth Surface Processes and Landforms*, v. 30, p. 985–1006, doi: 10.1002/esp.1258.
- Trumbore, S.E., Chadwick, O.A., and Amundson, R., 1996, Rapid exchange between soil carbon and atmospheric carbon dioxide driven by temperature change: *Science*, v. 272, p. 393–396, doi: 10.1126/science.272.5260.393.
- von Blanckenburg, F., 2006, The control mechanisms of erosion and weathering at basin scale from cosmogenic nuclides in river sediment: *Earth and Planetary Science Letters*, v. 242, p. 224–239, doi: 10.1016/j.epsl.2005.11.017.
- Wallbrink, P.J., and Murray, A.S., 1993, Use of fallout radionuclides as indicators of erosion processes: *Hydrological Processes*, v. 7, p. 297–304, doi: 10.1002/hyp.3360070307.
- West, J.A., Galy, A., and Bickle, M., 2005, Tectonic and climatic controls on silicate weathering: *Earth and Planetary Science Letters*, v. 235, p. 211–228, doi: 10.1016/j.epsl.2005.03.020.
- White, A.F., and Blum, A.E., 1995, Effects of climate on chemical weathering in watersheds: *Geochimica et Cosmochimica Acta*, v. 59, p. 1729–1747, doi: 10.1016/0016-7037(95)00078-E.
- White, A.F., and Brantley, S.L., 2003, The effect of time on the weathering of silicate minerals: Why do weathering rates differ in the laboratory and field?: *Chemical Geology*, v. 202, p. 479–506, doi: 10.1016/j.chemgeo.2003.03.001.
- Yoo, K., Amundson, R., Heimsath, A.M., Dietrich, W.E., and Brimhall, G.H., 2007, Integration of geochemical mass balance with sediment transport to calculate rates of soil chemical weathering and transport on hillslopes: *Journal of Geophysical Research*, v. 112, F02013, doi: 10.1029/2005JF000402.

Manuscript received 19 January 2009

Revised manuscript received 9 June 2009

Manuscript accepted 9 June 2009

Printed in USA